Volume 12, Year 2025 ISSN: 2564-4998

DOI: 10.11159/jbeb.2025.006

Repurposing Industrial Microscopy for Biology: Comparative Analysis of Cigarette Smoke-Induced Morphological Changes in Lung Epithelial Cells Using Keyence VHX-7000 and Zeiss Axiovert 200M

Sarah Li^{1,†}, Angie Sun^{1,†}, Yu-Sin (Jennifer) Ou², Huiying Huang¹, Wei Sun³, Veronica Gomez-Godinez¹, Linda Shi^{1,*}

¹Institute of Engineering in Medicine, University of California San Diego, La Jolla, CA, 92093

²School of Biological Science, University of California San Diego, La Jolla, CA, 92093

³UC San Diego Department of Medicine, La Jolla, CA, 92093

* Correspondence: zshi@ucsd.edu

†High school students participating in IEM OPALS program

Abstract - Cigarette smoke exposure induces oxidative stress, disrupts gene regulation, and causes morphological alterations in lung epithelial cells. While conventional methods such as qPCR and Western blotting are often used to study these effects, they are costly, labour-intensive, and unsuitable for rapid screening. In this study, we introduce a cost-effective imaging strategy to characterize early cellular responses of human bronchial epithelial cells (HBEpCs) to cigarette smoke extract (CSE). For the first time, the Keyence VHX-7000 digital microscope was employed to systematically analyse CSEinduced morphological changes, with direct comparison to the established Zeiss Axiovert 200M inverted fluorescence microscope. Quantitative analysis revealed consistent trends across both systems, demonstrating that the Keyence platform effectively captures morphological alterations with high throughput and minimal sample preparation. These findings establish the Keyence VHX-7000 as a viable, scalable alternative for preliminary cellular injury assessments, offering a practical tool for accelerating research into smoking-related lung and cardiovascular diseases.

Keywords: Cigarette Smoke Extract (CSE), Human Bronchial Epithelial Cells (HBEpCs), Keyence VHX-7000, Zeiss Axiovert 200M inverted fluorescence microscope, Morphological Analysis, Microscopy Comparison

© Copyright 2025 Authors - This is an Open Access article published under the Creative Commons Attribution License terms (http://creativecommons.org/licenses/by/3.0). Unrestricted use, distribution, and reproduction in any medium are permitted, provided the original work is properly cited.

1. Introduction

Chronic obstructive pulmonary disease, or COPD, represents one of the major global health issues, and its development is heavily associated with cigarette smoke. In fact, as of 2020, approximately 479 million people worldwide were affected by COPD, and that number is projected to increase nearly 50 percent by the year 2050 to 591 million. Inhaling smoke delivers thousands of toxic chemicals, such as nicotine and formaldehyde, into the airway and interacts with the lining epithelial cells, triggering symptoms such as chronic inflammation and oxidative stress, which can accumulate over time. While there are other risk factors, such as air pollution and dust exposure, that can contribute to the onset of COPD, smoking remains the most predominant cause. Other physiological reactions to smoke exposure can manifest narrowed. mucus-clogged bronchioles destruction of alveolar structures, resulting in impaired airflow and reduced gas exchange capacity. In terms of

Date Received: 2025-04-09 Date Revised: 2025-09-17 Date Accepted: 2025-10-01 Date Published: 2025-10-30 internal mechanism dysfunction, miRNA, which typically helps regulate cell function and maintain tissue health, is disrupted in ways that worsen disease. For example, some protective miRNAs that normally reduce inflammation become downregulated, while others that accelerate stress responses become overactive. This shift promotes chronic inflammation and impaired repair of airway cells, making the bronchial epithelium especially vulnerable to cigarette smoke. Further, Chen et al. identified mitophagy-related biomarkers in COPD, mitochondrial dysfunction to progression in cigarette smoke-exposed cells [1]. Dysfunctional mitophagy further exacerbates the disease by allowing damaged mitochondria to accumulate and generate reactive oxygen species, which can also damage DNA and proteins. Another majorly disrupted pathway worth mentioning would be the negative feedback loop for epithelial repair involving HHIP, in which excess exposure to cigarette smoke can contribute to disease progression. Chen et al. demonstrated that the COPD susceptibility gene HHIP regulates epithelial repair genes and maintains epithelial-mesenchymal unit integrity in response to cigarette smoke exposure [2]. This disruption causes HHIP to be unable to properly regulate inflammatory growth hormones, leading to abnormal wound healing in which the pathway is unable to properly rehabilitate epithelial cells and tissues. However, Chen et al. also showed that N-acetyl-L-cysteine protects lung tissues and alveolar epithelial cells from cigarette smokeinduced oxidative stress by reducing cellular injury [3]. Additionally, Huang et al. found that dietary zinc activates the Nrf2 signalling pathway to inhibit pyroptosis and attenuate lung inflammation in a COPD model [4]. Together, these processes begin at the level of bronchial epithelial cells, which is the focal point of this study.

In fact, recent studies have increasingly utilized human bronchial epithelial cells (HBEpCs) to investigate molecular mechanisms underlying airway diseases. For example, Myszor et al. uncovered critical pathways involved in airway innate immunity [5], Gao et al. studied lung cell apoptosis during pneumonia [6], and Yue et al. explored sepsis-induced lung injury and its impact on lung epithelial apoptosis [7]. As shown within these studies, HBEpCs have been popularized in the context of studying lung cell changes due to injury-inducing exposures.

Our project focuses on investigating how cigarette smoking-induced oxidative stress alters the behavior of

microRNAs (miRNAs) within these HBEpCs, shifting its role from cellular protection to promoting disease.

Traditionally, these investigations relied on molecular biology techniques such as quantitative PCR (qPCR), Western blotting, and immunofluorescence microscopy to assess changes in gene expression, protein abundance, and apoptosis markers under disease-related conditions. While these methods are highly sensitive and regarded as gold standards, they are also expensive, time-consuming, and labor-intensive, requiring costly reagents, specialized equipment, and multi-step workflows that are prone to technical variability.

To address this challenge efficiently, we explored, for the first time, the use of the Keyence VHX-7000 highresolution digital microscope to study the effects of CSE on HBEpCs. Given its cost-effectiveness, ease of use, and ability to rapidly capture high-resolution images, the Kevence system offers a promising alternative to traditional biological imaging platforms. To assess its performance, we directly compared the imaging results and morphological measurements obtained from the Keyence VHX-7000 with those from the widely used Zeiss Axiovert 200M inverted fluorescence microscope. By systematically evaluating the comparability and limitations of the Keyence system, we aim to establish its utility for studying smoking-induced cellular injury, providing a more accessible option for future lung and heart disease research.

The Keyence VHX-7000 is primarily used in semiconductor and industrial inspection, producing high-contrast images of ball grid arrays, MEMS devices, wire bonds, and metal pads. Its strengths lie in rapid imaging, wide field-of-view capture, and the ability to detect small surface imperfections. While the Keyence VHX-7000 has been successfully utilized in industrial and material science research fields such as coating characterization [8], surface wear analysis [9], and optical surface finishing [10], its application for biological cell imaging has been largely unexplored.

In contrast, Zeiss Axiovert microscopes have long been regarded as gold standards for high-resolution imaging in biological and medical research [11-12]. The Zeiss Axiovert serves as the benchmark in our study because it provides comprehensive imaging capabilities essential for detecting subtle cellular changes. Z-stacking allows acquisition of multiple optical slices through cells, enabling precise 3D reconstruction and detailed analysis of internal structures. In addition to Z-stacking, other key features include 3D shadow projection which adds depth

and helps to visualize morphology in thick samples. Fluorescence capabilities, including DAPI staining, allow observation of nuclei, cytoskeleton, and proteins. These capabilities make Zeiss ideal for high-resolution, multiparameter analysis, and any comparative study using Keyence must be interpreted against this rich dataset.

By adapting a commercially available Keyence VHX-7000 system for morphological analysis of HBEpCs, we introduce a cost-effective, high-throughput alternative to conventional biological imaging methods, and directly compare its capabilities and limitations against the established Zeiss Axiovert 200M platform. Our hypothesis was that if Keyence can reveal micro-scale defects in electronics, it may also detect subtle cellular changes, such as nuclear enlargement or membrane blebbing, after CSE exposure.

2. Materials and Methods

For our materials, we cultured cryopreserved human bronchial epithelial cells and exposed them to either 0.3% DMSO as a control or 0.3% cigarette smoke extract, an aqueous solution dervied from cigarette smoke. Treatments were applied for 10, 30, 60, and 90 minutes to capture temporal dynamics in cellular response. This design allowed us to assess both immediate and delayed morphological changes, providing insight into the kinetics of smoke-induced injury.

2.1 Cell Preparation

Cryopreserved primary HBEpCs were obtained from Cell Applications, Inc. (Catalog #CA-502-05a) and cultured at 37°C with 5% $\rm CO_2$ in HBEpC/HTEpC growth medium (Catalog #CA-511K). Cells between passages 3 and 11 were used for all experiments.

For treatments, cells were exposed to 0.3% CSE (Murty Pharmaceuticals, Catalog #MPI-250311) by adding 1.5 μ L of CSE to 500 μ L of culture medium. Parallel control groups were treated with 0.3% dimethyl sulfoxide (DMSO; Millipore Sigma, Catalog #D2650) at the same dilution. Fixation times were set at 10, 30, 60, and 90 minutes.

2.2 Cell Fixation and Staining

Following exposure, cells were fixed to preserve structural integrity and stained to highlight nuclei for visualization. This step was critical because the two imaging systems rely on different detection principles. Keyence primarily captures contrast-based morphology,

so fixed cells offer consistent imaging conditions. Zeiss, on the other hand, combines phase contrast with fluorescence, and fixation preserves both cytoplasmic and nuclear detail. Standardizing fixation and staining allowed us to fairly compare the platforms' performance and evaluate their relative sensitivity to cigarette smoke-induced changes. The cells were fixed and stained using the following procedure, as shown in Figure 1.:

- 1. Allow glutaraldehyde solution to equilibrate to room temperature.
- 2. Remove culture medium and wash cells three times quickly with phosphate-buffered saline (PBS).
- 3. Fix cells in 200 μL of 0.25% glutaraldehyde in PBS for 3 minutes at room temperature.
- 4. Wash cells three times with PBS and maintain them in 1 mL of PBS.
- 5. Seal dishes with parafilm to prevent evaporation if fixation is paused.
- 6. Incubate cells with 200 μL of 50 mM glycine solution for 5 minutes to quench residual glutaraldehyde.
- 7. Add one drop of NucBlue Live ReadyProbes reagent (Thermo Fisher Scientific) for nuclear staining and incubate in the dark for 5 minutes.
- 8. Wash three times with PBS, disposing of waste in a designated PFA container under a chemical hood.
- 9. Apply one drop of mounting medium (prewarmed to room temperature) and carefully place a coverslip without introducing bubbles.
- 10. Incubate overnight in the dark before transferring to refrigeration for storage.

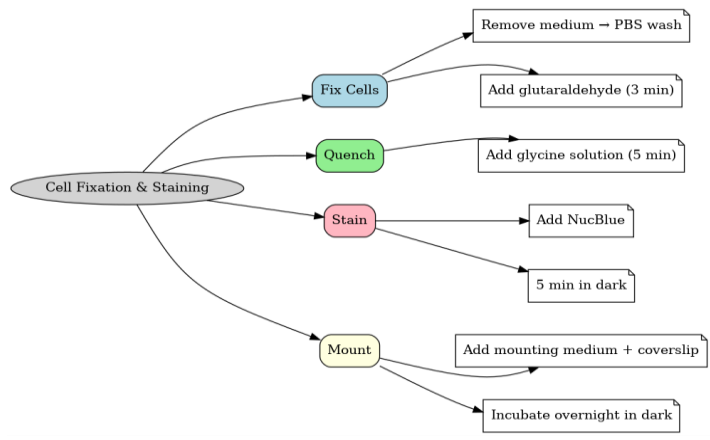


Figure 1. Lung cell fixation and staining process categorized into four main components: fixing, quenching, staining, and mounting.

2.3 High-Resolution Digital Imaging Platforms

In this study, two imaging systems were utilized to characterize the morphological changes in HBEpCs following CSE exposure:

Keyence VHX-7000: It integrates optics, camera, LED illumination, motorized stage, and image processing software into a single system. Features such as high dynamic range (HDR) imaging and real-time depth composition enable fully focused, high-contrast images across irregular surfaces. While traditionally applied to non-biological samples, this system was evaluated for the first time here to monitor large-scale morphological changes in human epithelial cells. The two standout capabilities from Keyence Microscope:

- Automatic Focusing and Stitching: In semiconductor applications, this function is widely used to keep entire three-dimensional structures such as ball grid arrays (BGAs), MEMS devices, wire bonds, and uneven metal pads in sharp focus while stitching multiple fields into a single composite image. In the biological setting, we leveraged this same capability to image confluent sheets of lung epithelial cells, maintaining clarity across uneven monolayers and capturing subtle morphological changes such as swelling, elongation, or detachment.
- Automatic Quantitative Evaluation: For electronic materials, this tool is typically used to quantify features like the height of solder balls in BGAs, the thickness of MEMS membranes, the integrity of wire bonds, or the flatness of metal pads. In our study, we adapted this function to extract quantitative metrics of lung cell morphology, including cell area, height variation, and surface roughness, enabling unbiased measurement of structural changes induced by experimental conditions.

Zeiss Axiovert 200M: A research-grade inverted fluorescence microscope extensively used in biomedical studies for live-cell imaging, fluorescence microscopy, and high-resolution visualization of cellular structures. It supports a variety of imaging modes (e.g., fluorescence, DIC, phase contrast) and is optimized for biological

sample imaging, making it a gold standard for cellular research.

Table 1 lists the comparison of the features of the two systems. When directly comparing the Keyence VHX-7000 and Zeiss Axiovert 200M, several key differences emerge in both imaging capabilities and the type of biological information each platform can provide. Zeiss excels in high-resolution phase contrast and fluorescence imaging, enabling detailed visualization of subcellular structures, notably the nucleus and cytoplasm. This allows precise measurement of cell area. nuclear size, circularity, and membrane blebbing frequency. It also captures heterogeneity within the cell population, revealing that not all cells respond synchronously to cigarette smoke exposure, as some cells show early stress responses while others display delayed responses. On the other hand, Keyence primarily relies on contrast-based imaging, providing excellent throughput and wide-field capture but limited cytoplasmic resolution. Because of this, Keyence may not be able to detect fine features such as cytoplasmic vacuolization, subtle blebs, or early-stage heterogeneity are less visible. However, given its lower cost and easier accessibility, combined with a general ease of use, exploring the potential of Kevence microscopy in biological fields may prove to be a potential costeffective way to study lung cells without significantly compromising morphological detection capabilities.

Table 1. Comparison of Keyence VHX-7000 and Zeiss Axiovert 200M for Lung Cell Imaging.

Feature/Use Case	Keyence VHX- 7000	Zeiss Axiovert 200M
Cost and Accessibility	Cost-effective	Higher cost
Ease of Use	Highly automated	Requires technical Expertise
High-Resolution Imaging	Excellent	Excellent
Biological Live Cell Imaging	Not suitable	Excellent
Fluorescence Imaging	Not suitable	Excellent
Z-Stacking	Built-in	Possible with accessories

Feature/Use Case	Keyence VHX-	Zeiss Axiovert
	7000	200M
Sample		
Preparation	Minimal	Demanding
Requirements		
Wide Field of View	Large-scale	Good but
	Capture	more localized

3. Results and Discussions

3.1 Morphological Analysis of HBEpCs Using the Keyence VHX-7000 System

This study represents the first systematic application of the Keyence VHX-7000 platform to characterize CSE-induced morphological changes in HBEpCs. The Keyence system, using uniform LED illumination and HDR imaging, allowed acquisition of detailed, high-contrast images for rapid visualization of cell nucleus outlines against background substrates. HDR processing further enhanced feature visibility, supporting precise cell size quantification from a single wide-field image that captured hundreds of cells at once. Real-time depth composition was utilized to combine multiple focal planes into fully focused composite images, overcoming the challenges of uneven sample surfaces and enabling clear identification of subtle structural changes and damage induced by CSE treatment. This imaging strategy enabled highthroughput, non-destructive, cost-effective assessment across eight experimental groups: 0.3% CSE or 0.3% DMSO across four time points (10, 30, 60, and 90 minutes). Two imaging modes were utilized: Enhanced Contrast and Enhanced Flaw Detection (Figure 2), allowing clear visualization of cellular boundaries and detection of subtle structural alterations.

Quantitative measurement of the long axis of individual cell nucleus was performed using ImageJ and revealed no statistically significant difference in nucleus size between the CSE and DMSO groups at the 10-, 30-, and 60-minute time points (p > 0.05, one-way ANOVA with Tukey's post hoc test). However, as shown in Figure 3, at 90 minutes, CSE-treated cells exhibited a significant change in nucleus size compared to DMSO controls (p = 0.037, one-way ANOVA with Tukey's post hoc test; n = 25 per group. The mean \pm standard deviation values were 16.0 ± 3.23 and 19.6 ± 3.77 , respectively). This suggests that prolonged exposure to CSE induces measurable morphological changes in epithelial cells, which are detectable using the Keyence platform.

The enlarged nuclei observed after 90 minutes are consistent with known smoke-induced stress responses.

Nuclear swelling has been linked to early stages of oxidative stress and DNA damage, which can trigger apoptotic pathways. In the context of cigarette smoke exposure, excessive reactive oxygen species (ROS) can damage mitochondrial DNA and proteins, impairing mitophagy and leading to further accumulation of dysfunctional mitochondria [13]. This cycle not only promotes apoptosis but also disrupts miRNA regulation, reducing protective miRNAs and upregulating proinflammatory ones. Additionally, impaired HHIP signalling limits epithelial repair capacity, further exacerbating cellular injury [14]. Thus, the changes we observed, particularly enlargement, likely reflect early symptoms of oxidative stress and a progression toward apoptosis in bronchial epithelial cells.

The ability to efficiently capture and analyze hundreds of cells in a single field of view highlights the Keyence system's high-throughput advantage. Its HDR and real-time depth composition features proved effective in resolving morphological features even in slightly uneven culture surfaces.

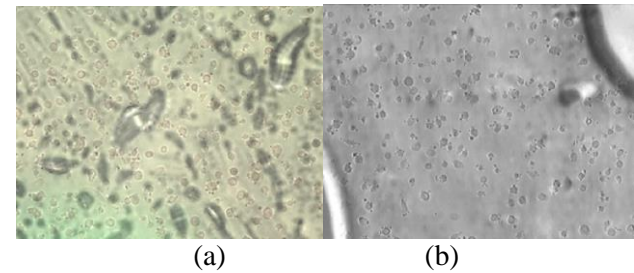


Figure 2. Keyence Imaging with Enhanced Contrast (a) and Enhanced Flaw (b).

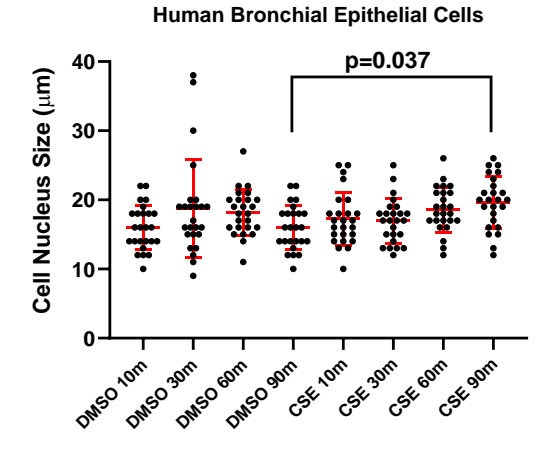


Figure 3. Statistical study of the cell nucleus size using the images captured by VHS 7000. Data are presented as mean ±

standard deviation. P values were calculated using one-way ANOVA with Tukey's post hoc test. n = 25 for each group.

3.2 Morphological Analysis of HBEpCs Using Zeiss Axiovert 200M Microscopy

Parallel imaging was performed using the Zeiss Axiovert 200M inverted fluorescence microscope. Cells were visualized using both Phase 3 imaging and Blue Fluorescence Protein (BFP) fluorescence channels to capture morphology and DAPI-stained nuclei, respectively (Figure 4).

Quantitative measurements of the long axis in both phase and fluorescence images were performed using ImageJ. Statistical analysis (Figure 5) revealed comparable findings to those obtained with the Keyence system: minimal differences between CSE and DMSO groups at earlier time points, but significant size changes of cells in the CSE group after 90 minutes.

Notably, measurements from the Zeiss BFP images, which mainly captured nuclear size due to thin cytoplasmic membranes, aligned well with the Keyence measurements. This cross-validation strengthens the reliability of the morphological observations and confirms that both imaging systems, despite differences in optics and sample illumination, captured consistent biological trends.

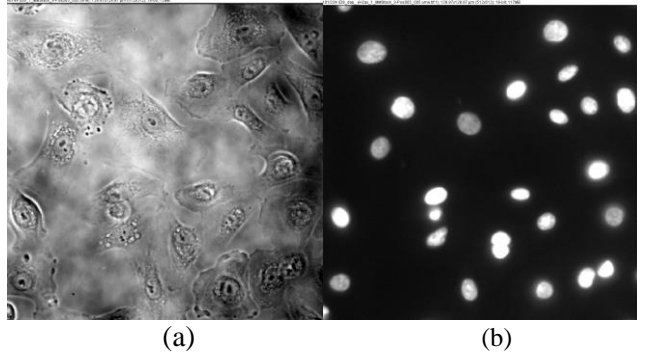


Figure 4. Images captured under Zeiss Axio 200M Microscope (a) under Phase 3, (b) BFP DAPI image of (a).

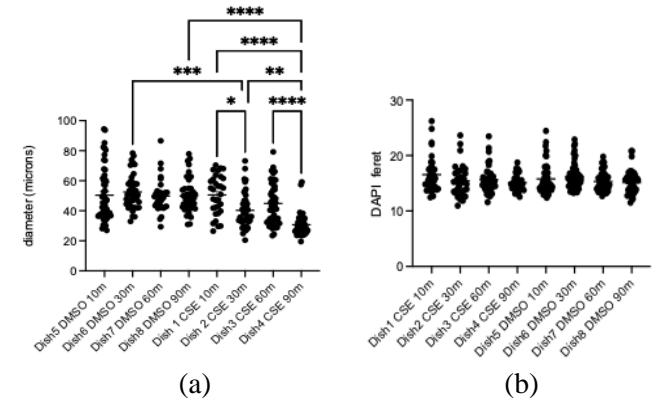


Figure 5. Statistical studies of the cell morphology changes by Zeiss Axio 200M: (a) cell size measurement under Phase 3, (b) Nucleus size measurement under BFP (DAPI image) Data presented as mean \pm standard deviation. P values were calculated using one-way ANOVA with Tukey's post hoc test. n = 25 for each group. *: p < 0.05, **: p < 0.01, ***: p < 0.001, ****: p < 0.0001. The number of cells for each dish were: 34 for Dish1, 41 for Dish 2, 4, 6, 49 for Dish 3, 57 for Dish 5, 33 for Dish 7, and 40 for Dish 8.

4. Conclusion

This study represents the first systematic transformation of the Keyence VHX-7000 from its traditional role in semiconductor inspection to a biological research tool for monitoring cigarette smoke-induced injury in human bronchial epithelial cells. By adapting a microscope originally designed to evaluate ball grid arrays, MEMS devices, wire bonds, and metal pads, we demonstrated that the Keyence can be repurposed to capture hallmark cellular alterations such as change in nucleus size and detachment of cells following CSE exposure. Critically, these measurements closely aligned with those obtained using the gold-standard Zeiss Axiovert 200M system, establishing the feasibility of translating industrial imaging technologies into biomedical applications.

Future work will expand sample sizes to strengthen statistical correlation with Zeiss-based measurements, incorporate additional morphological and viability parameters, and examine both dose- and time-dependent responses to CSE.

Beyond cigarette smoke injury, concrete next steps include: testing the platform with other inhaled toxins such as diesel exhaust particles, wildfire smoke, or e-cigarette vapor to determine whether distinct morphological signatures emerge; applying the system to live-cell imaging of epithelial barrier integrity and wound healing assays, which would assess dynamic processes like cell migration and detachment in real

time; and extending the approach to other epithelial tissues, including nasal, gastrointestinal, and even vascular endothelium, to evaluate how diverse cell types respond to environmental stressors. These applications would demonstrate the broader utility of the Keyence platform as a cost-effective, high-throughput imaging tool for both toxicological screening and general biomedical research.

Acknowledgements

This material was based upon work supported by a gift from Beckman Laser Institute Inc. to L.S. and V.G.G.. Special thanks to the private donors to our UCSD IEM BTC center: Dr. Shu Chien from UCSD Bioengineering, Dr. Lizhu Chen from CorDx Inc., Dr. Xinhua Zheng, David & Leslie Lee, Mingwei He and Wen Shi for their generous donations.

References

- [1] Chen J, Zhang X, Sun G. Identification and validation of biomarkers related to mitophagy in chronic obstructive pulmonary disease. Mol Med Rep. 2025 Apr;31(4):93. doi: 10.3892/mmr.2025.13458. Epub 2025 Feb 14. PMID: 39950319; PMCID: PMC11843435.
- [2] Chen Q, Wisman M, Nwozor KO, Sin DD, Joubert P, Nickle DC, Brandsma CA, de Vries M, Heijink IH. COPD susceptibility gene HHIP regulates repair genes in airway epithelial cells and repair within the epithelial-mesenchymal trophic unit. Am J Physiol Lung Cell Mol Physiol. 2025 Apr 7. doi: 10.1152/ajplung.00220.2024. Epub ahead of print. PMID: 40192657.
- [3] Chen J, Cheng Y, Cui H, Li S, Duan L, Jiao Z. Nacetyl-L-cysteine protects rat lungs and RLE-6TN cells from cigarette smoke-induced oxidative stress. Mol Med Rep. 2025 Apr;31(4):97. doi: 10.3892/mmr.2025.13462. Epub 2025 Feb 21. PMID: 39981906; PMCID: PMC11865697.
- [4] Huang Y, Liang T, Liu J, Yu H, Li J, Han L. Dietary Zinc activates the Nrf2 signaling pathway to inhibit pyroptosis and attenuate the lung inflammatory response in COPD. Cytotechnology. 2025 Apr;77(2):62. doi: 10.1007/s10616-025-00725-7. Epub 2025 Feb 18. PMID: 39980839; PMCID: PMC11836256.
- [5] Myszor IT, Lapka K, Hermannsson K, Rekha RS, Bergman P, Gudmundsson GH. Bile acid metabolites enhance expression of cathelicidin antimicrobial peptide in airway epithelium through activation of the TGR5-ERK1/2 pathway. Sci Rep. 2024 Mar

- 21;14(1):6750. doi: 10.1038/s41598-024-57251-3. PMID: 38514730; PMCID: PMC10957955.
- [6] Gao P, 12 J, Jiang M, Li Z, Xu D, Jing J, Yihepaer, Hu T. LncRNA SNHG16 is Downregulated in Pneumonia and Downregulates miR-210 to Promote LPS-Induced Lung Cell Apoptosis. Mol Biotechnol. 2023 Mar;65(3):446-452. doi: 10.1007/s12033-022-00545-6. Epub 2022 Aug 22. PMID: 35994228.
- [7] Yue C, He M, Teng Y, Bian X. Long non-coding RNA metastasis-related lung adenocarcinoma transcript 1 (MALAT1) forms a negative feedback loop with long non-coding RNA colorectal neoplasia differentially expressed (CRNDE) in sepsis to regulate lung cell apoptosis. Bioengineered. 2022 Apr;13(4):8201-8207. doi: 10.1080/21655979.2021.2023727. PMID: 35300579; PMCID: PMC9161944.
- [8] Dudek, A., & Kierat, O. (2024). Preliminary Aspects Regarding the Anticorrosive Effect of Multi-Layered Silane–Hydroxyapatite Coatings Deposited on Titanium Grade 2 for Medical Applications. Materials, 17(23), 6001. https://doi.org/10.3390/ma17236001.
- [9] Stradomski, G., Fik, J., Lis, Z., Rydz, D., & Szarek, A. (2024). Wear Behaviors of the Surface of Duplex Cast Steel after the Burnishing Process. Materials, 17(8), 1914. https://doi.org/10.3390/ma17081914.
- [10] Shrotri, A., Preu, S., & Stübbe, O. (2025). Achieving Transparency and Minimizing Losses of Rough Additively Manufactured Optical Components by a Dip-Coating Surface Finish. Coatings, 15(2), 210. https://doi.org/10.3390/coatings15020210.
- [11] Dorn A, Zappe H, Ataman Ç. Conjugate adaptive optics extension for commercial microscopes. Advanced Photonics Nexus. 2024 Sep 1;3(5):056018-.
- [12] Wang, P., Liang, J., Shi, L.Z., Wang, Y., Zhang, P., Ouyang, M., Preece, D., Peng, Q., Shao, L., Fan, J. "Visualizing Spatiotemporal Dynamics of Intercellular Mechanotransmission upon Wounding." ACS Photonics 2018, 5, 3565–3574. https://doi.org/10.1021/acsphotonics.8b00383.
- [13] Guo, C., Sun, L., Chen, X., Zhang, D. "Oxidative stress, mitochondrial damage and neurodegenerative diseases." *Neural regeneration research* vol. 8,21 (2013): 2003-14. doi:10.3969/j.issn.1673-5374.2013.21.009
- [14] Deritei, Dávid et al. "HHIP's Dynamic Role in Epithelial Wound Healing Reveals a Potential Mechanism of COPD Susceptibility." *bioRxiv : the preprint server for biology* 2024.09.05.611545. 8 Oct. 2024, doi:10.1101/2024.09.05.611545.